Supplementary Information

Mechanistic Understanding of Efficient Electrocatalytic Hydrogen Evolution Reaction on 2D Monolayer WSSe Janus Transition Metal Dichalcogenide

Vikash Kumar[1] and Srimanta Pakhira[1,2*]

[1] Theoretical Condensed Matter Physics and Advanced Computational Materials Science Laboratory, Department of Physics, Indian Institute of Technology Indore, Simrol, Khandwa Road, Indore-453552, MP, India.

[2] Theoretical Condensed Matter Physics and Advanced Computational Materials Science Laboratory, Centre for advanced Electronics (CAE), Indian Institute of Technology Indore, Simrol, Khandwa Road, Indore-453552, MP, India.

*Corresponding author: spakhira@iiti.ac.in (or) spakhirafsu@gmail.com

S1- Theoretical Calculations and equations

Here, it is important to calculate the change in Gibbs free energy (ΔG) in between intermediates states for the HER mechanism. So, the Gibbs free energy (G) for each HER step was calculated at 298.15 K by the following equation:

$$G = E_{DFT} + E_{ZPE} + \int C_p dT - TS$$

Where E_{DFT} is the electronic energy, E_{ZPE} is the zero-point energy, $\int C_P dT$ is the enthalpic temperature correction, and TS is the entropic contribution. E_{ZPE}, $C_P dT$, and TS are calculated from temperature, pressure, and calculated vibrational energy using the standard DFT method. The catalytic performances of the 2D monolayer Janus WSSe were characterized by the calculations of the changes of free energy (ΔG), enthalpy (ΔH), and electronic energy (ΔE) for all the reactant, products, intermediates, and TSs for the HER.

Change of free energy: $$\Delta G = \sum G_{Product} - \sum G_{Reactant}$$

Change of enthalpy: $$\Delta H = \sum H_{Product} - \sum H_{Reactant}$$

Change of electronic energy: $$\Delta E = \sum E_{Product} - \sum E_{Reactant}$$

For all purposes, we considered standard hydrogen electrode (SHE) conditions, where electrons and protons (pH = 0) are in equilibrium with 1 atmosphere of H_2. In other words, the energy of the H^+/e^- pair is equal to half of the gaseous hydrogen (i.e., $0.5H_2$) at equilibrium potential.

S2- Electronic and structural properties

Table S1: The equilibrium lattice parameter (a), bond distance (d), bond angles, and Band gap (E_g) of the 2D monolayer pristine WS_2, WSe_2, and Janus WSSe are summarized here.

Materials	**Lattice parameter (in Å)**	**Bond distance (in Å)**	**Bond angle (in °)**	**Band gap (in eV)**	**References**
WS_2	3.14	W-S= 2.39	α = β=90 γ = 120	2.78	This work
WS_2 (Previously reported)	3.16	W-S=2.45	α = β=90 γ = 120	2.88	[1,2]
WSe_2	3.22	W-Se=2.50	α = β=90 γ = 120	2.39	This work
WSe_2 (Previously reported)	3.29	W-Se=2.53	α = β=90 γ = 120	2.42	[1,2]
WSSe	3.19	W-S=2.40, W-Se=2.49	α = β=90 γ = 120	2.64	This work

WSSe (Previously reported)	3.26	W-S=2.42, W-Se=2.54	α = β=90 γ = 120	2.68	3

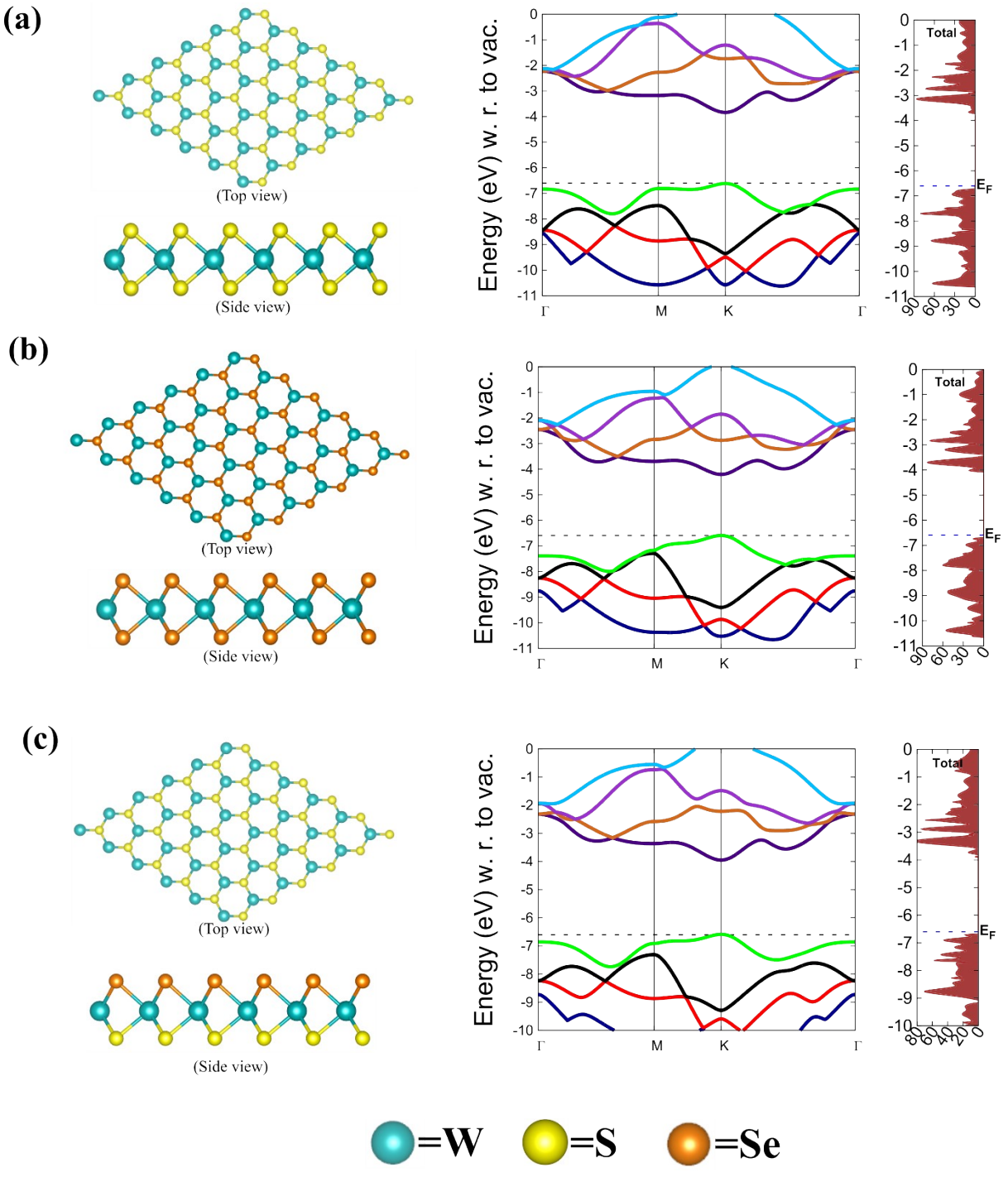

Figure S1. (a) The top view and the side view representation of 2D monolayer WS_2 with the band structure and total density of states (DOS). (b) The top view and the side view of 2D monolayer WSe_2 with the band structure and total density of states. (c) The top view and the side view of 2D monolayer Janus WSSe with the band structure and the total density of states are shown here.

S3 Cluster Model Validation

In order to verify the molecular cluster model system $W_{10}S_{12}Se_9$ which has the same chemical/electronic properties as the W-edge of the 2D monolayer WSSe JTMD, we calculated the hydrogen adsorption energies for both the molecular cluster model and periodic 2D monolayer WSSe JTMD. Figure S2 shows that the hydrogen binding energies determined by using the finite clusters and 2D periodic slabs differ by an amount of 0.09 eV and 0.21 eV for the two different stoichiometries. This cluster model $W_{10}S_{12}Se_9$ has been developed to explore and investigate the electrochemical reaction mechanisms with the most favorable H_2 evolution reaction pathway, as it allows for more flexible use of the M06-L DFT method, which more precisely determines reaction barriers, reaction kinetics, intermediates, and bond energies. It is difficult to use a cluster model with a net charge in the case of periodic systems, i.e., it is not possible to consider the charge of the system during the subject reaction in the 2D periodic model system of the WSSe JTMD. Furthermore, the cluster model allows us to incorporate electrons (e^-) and protons (H^+) simultaneously into various reaction steps and report free energy as a function of electrochemical potential and pH. Very recently, Pakhira et al. studied the electrocatalytic activities of the 2D single-layer MoSSe JTMD where they used similar kinds of molecular cluster model system to investigate the electrocatalytic HER on the surfaces of MoSSe JTMD.[4] The present $W_{10}S_{12}Se_9$ molecular cluster model has the same chemical properties as the periodic 2D Janus WSSe, as depicted in Figure S2.

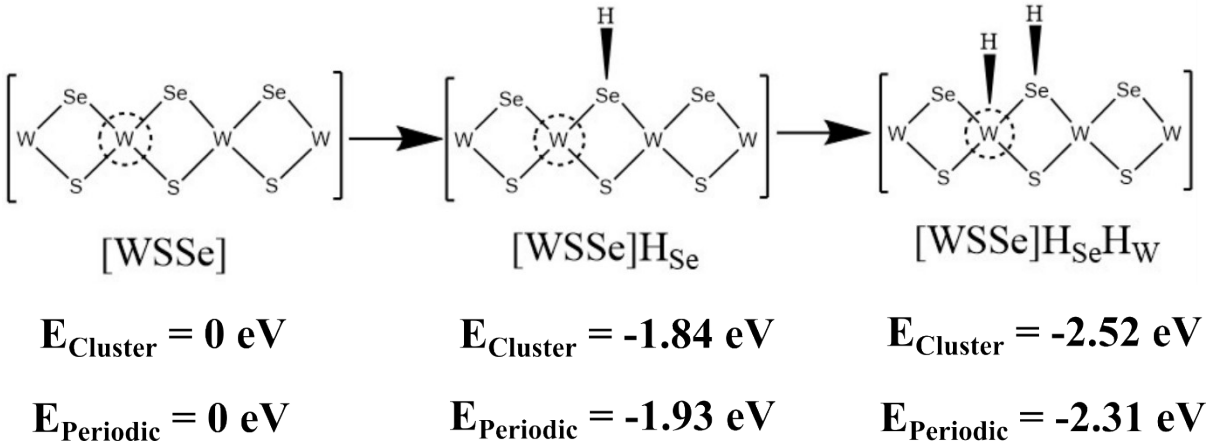

Figure S2. Hydrogen adsorption energy at the W-edge of 2D monolayer WSSe JTMD. $E_{Cluster}$ represents the relative electron energy during hydrogen adsorption considering the molecular cluster model system, and $E_{Periodic}$ is the relative electron energy obtained from periodic 2D layer calculations.

We calculated the hydrogen adsorption energies of 2D WS_2 and WSe_2 periodic structures for comparison with 2D monolayer WSSe JTMD. In pristine 2D monolayers, WS_2 and WSe_2 hydrogen adsorption energy have been found at -2.23 eV and -2.59 eV, respectively. However, in 2D monolayer Janus WSSe, hydrogen adsorption has been found at -1.93 eV. We need a catalyst for hydrogen production that has hydrogen adsorption energies approximately equal to zero. Therefore, the hydrogen adsorption energy of the catalyst should appear as close to zero as possible. So, here we show that the hydrogen adsorption energy of the 2D Janus WSSe is close to zero compared to other pristine materials (WS_2 and WSe_2). Then 2D Janus WSSe excellent electrocatalyst for hydrogen production because of its less hydrogen adsorption energy than pristine WS_2 and WSe_2 materials.

S4- Tafel mechanism and S-terminal W-edge of 2D monolayer WSSe JTMD material for HER

In this study, we have also investigated the Volmer-Tafel reaction mechanism for HER to compare the reaction performances and thermodynamic stability with the Volmer-Heyrovsky mechanism. The reaction pathway, reaction thermodynamics, kinetics, and reaction energy constraints of H_2 formation are examined considering the Vollmer-Tafel HER mechanism considering the molecular cluster model system $W_{10}S_{12}Se_9$ of the 2D monolayer WSSe JTMD. The equilibrium geometry, intermediate and transition state (TS) of the Vollmer-Tafel mechanism have been calculated by the same M06-L DFT method and are shown in Figure 4a-g and Figure S3. However, to move the H atoms on the two neighboring Se and W atoms towards a potential transition state (TS3), known as the Tafel transition state (noted by TS3), is found in the present study, as depicted in Figure S3. In other words, $[WSSe]H_WH_{Se}$ has two H atoms which react with each other through a potential transition state called the Tafel TS3. Harmonic vibrational calculations indicate that TS3 has a single imaginary frequency about -485.27 cm^{-1} before forming H_2 during Tafel HER. The reaction barrier (ΔG) obtained by the M06-L DFT method was found to be 10.02 $kcal.mol^{-1}$, which is higher than the previous intermediate $[WSSe]H_{Se}H_W$. The changes in the electronic energy (ΔE) and enthalpy (ΔH) of the Tafel TS3 in this Volmer-Tafel reaction phase are shown in Table 2. Therefore, these calculations suggest that the Volmer-Tafel reaction mechanism is thermodynamically less favorable for the evolution of H_2 than the Volmer-Heyrovsky reaction mechanism.

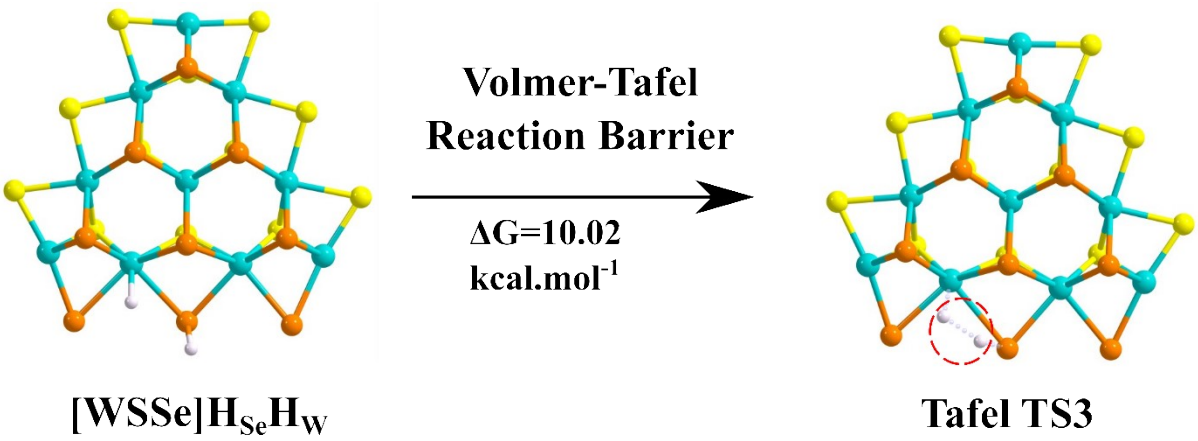

Figure S3. Equilibrium geometries of the $[WSSe]H_{Se}H_W$ and Tafel transition state TS3 occurred during the Volmer-Tafel reaction step with the change in the free energy (i.e., relative free energy or reaction barrier ΔG) about 10.02 kcal.mol^{-1} computed in the gas phase are depicted here.

Considering the same cluster model system $W_{10}S_{12}Se_9$, further examinations have been carried out to investigate the electrocatalytic activity of the S-terminal W-edge of 2D monolayer WSSe JTMD material for HER. By considering the S-terminal W-edge of the 2D monolayer WSSe material, the same H_2 evolution reaction pathway has been investigated (as shown in Figure 4e) contemplating the similar finite clustering model system $W_{10}S_{12}Se_9$. Equilibrium geometries of the important intermediates and transition states involved in the subject reaction, $[WSSe]H_S$ and TS4 (H*-migration), are displayed in Figure S4, as they play an important role in determining the performance of electrocatalytic activity for efficient HER. The present DFT-D calculations found that the H*-migration reaction barrier (ΔG) is approximately 2.94 kcal.mol^{-1} when reacted at the S-terminated W-side of the 2D monolayer WSSe JTMD material. The reaction barrier of the TS4 was approximately 0.61 kcal.mol^{-1} higher than that TS1 of the Se-terminated W-edge of the 2D WSSe JTMD material, indicating that the S-terminated W-edges of the 2D monolayer WSSe JTMD is thermodynamically less favorable for HER compared to the Se-terminated W-edges during the HER process. It has been recently reported that the Se-terminated Metal-edges of the 2D monolayer JTMD are thermodynamically favorable than S-terminated Metal-edges during the HER process.[4] The present investigation also shows that the HER process at the S-terminal W-edge of the 2D WSSe JTMD is less thermodynamically favorable than the Se-terminal W-edge.

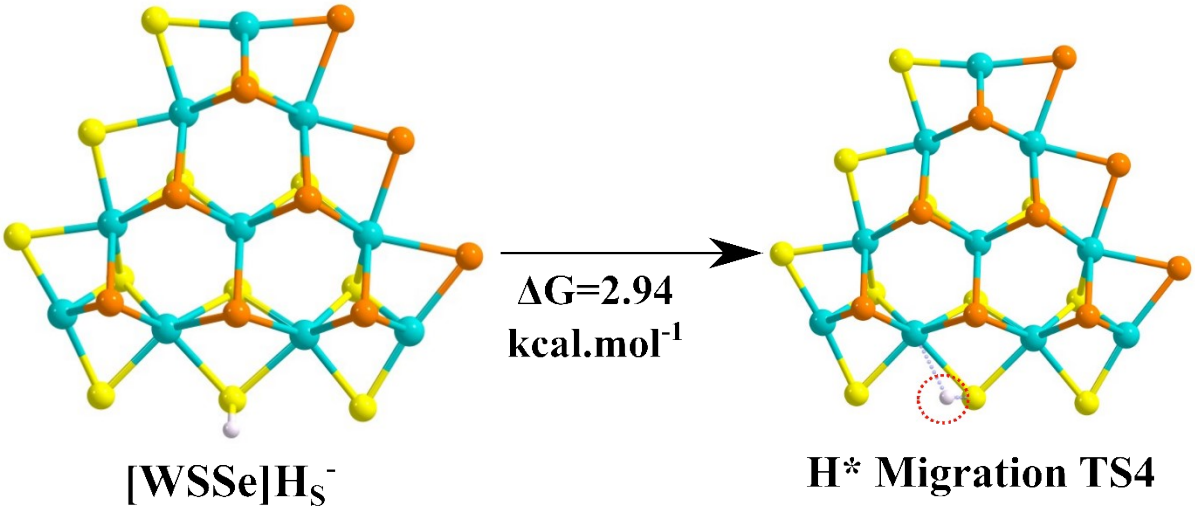

Figure S4. The equilibrium geometry of the S-edge: $[WSSe]H_S^-$ and TS4 (H*-migration transition states) have been calculated by the M06-L DFT method. The HER occurs at the S-terminal W-edge of the 2D monolayer WSSe JTMD surface.

S5- Turnover Frequency (TOF) and Tafel Slope calculations

To rank the electrocatalysts as per their catalytic activity, the turnover frequency (TOF)[5] corresponding to the quantity of H_2 released from each active site per unit time is another key parameter. According to the transition state theory (TST)[6] or activation recombination theory, we have determined the turnover frequency for the H_2 evolution at each edge of the W atom in the 2D WSSe JTMD catalyst. For the theoretical determination, we used the following formula:

$$rate = \frac{(k_B T)}{h} \times exp\left(-\frac{\Delta G}{RT}\right)$$

Where the symbol k_B represents the Boltzmann constant (1.381×10^{-23} J K^{-1}), T is the temperature in the absolute scale (here it is kept as a constant with an absolute scale value of 298.15 K throughout the non-periodic cluster model calculation), R is the universal gas constant (8.314 J mol^{-1} K^{-1}), h is the Planck's constant (6.623×10^{-34} J s^{-1}), and ΔG corresponds to the energy barriers. Our DFT-D study on the 2D single-layer Janus WSSe material found that the TOF at the edge of W is about 1.91×10^7 sec^{-1}, which corresponds to the activation energy barrier (ΔG ~ 7.52 kcal.mol^{-1}) during the Heyrovsky TS formation, i.e., TS2 at the W-edges. A higher TOF value is suitable for better H_2 production during the reaction. As shown in Table S2, the comparison of the activation energy and TOF of different TMD materials provides an understanding of their electrocatalytic activity and performance for effective HER.

We can observe that the 2D monolayer Janus WSSe material shows comparable results to the hybrid $W_{0.4}Mo_{0.6}S_2$ alloy material. However, the value of TOF is higher than the hybrid $W_{0.4}Mo_{0.6}S_2$ alloy material and other TMDs which indicates that the 2D monolayer Janus WSSe material is an excellent electrocatalyst for H_2 evolution. Therefore, what can be mentioned here is that the 2D monolayer WSSe material can prove to be a better and more practical alternative electrocatalyst to the catalytic performance of HER.

Table S2. The Heyrovsky reaction barriers and TOF for the 2D monolayer MoS_2, WS_2, $W_{0.4}Mo_{0.6}S_2$ alloy, Mn-MoS_2, and Janus WSSe material calculated at the theoretical level of the DFT method in the solvent phase are shown here.

Materials	**Barrier in the gas phase (ΔG) (kcal.mol^{-1})**	**Barrier in the solvent phase (ΔG) (kcal.mol^{-1})**	**Turnover frequency in solvent phase (Sec^{-1})**	**References**
MoS_2	16.0	23.8	2.1×10^{-5}	[7]
WS_2	14.5	21.3	1.5×10^{-3}	[7]
$W_{0.4}Mo_{0.6}S_2$	11.5	13.3	1.1×10^{3}	[7]
Mn-MoS_2	10.59	10.79	7.74×10^{4}	[8]
WSSe	5.05	7.52	1.91×10^{7}	This work

Another electrochemical parameter is the Tafel slope (***m***) which can be theoretically calculated based on the number of electrons transferred during the whole HER mechanism. Assuming that the rate of the catalyst is not confined by the electron directly transfer from the support to the desired catalyst, theoretically, the Tafel slope[5] (***m***) is given as $m = 2.303\left(\frac{RT}{nF}\right)$, where R = universal gas constant, T = absolute temperature which has constant value for our calculation, F = Faraday constant (96485 C mol^{-1}) and n is the number of electrons participating in the whole process. Tafel slope is an inverse measure of how strongly the reaction rate responds to changes in potential. It is used to evaluate the rate-determining steps during the HER generally assume extreme coverage of the adsorbed species. The lower values of both the activation energy barriers (both the H*-migration and Heyrovsky's reaction barrier energies) lead to the establishment of a sophisticated number of active sites by shrinking the value of

electrochemical properties like Tafel slope (***m***) and increasing the turnover frequency (TOF)[9-10] for an excellent catalytic activity to generate molecular hydrogen. As mentioned earlier, the proposed reaction is a two-electron transfer mechanism for the evolution of H_2 molecules, and it has been found that the calculated Tafel slope of this reaction occurred at the active edges of the 2D monolayer WSSe JTMD is about 29.54 mV dec^{-1} at T=298.15 K when n = 2.

S6- HOMO-LUMO Calculation

Through the visualization of the respective TS structures calculated by highest occupied molecular orbital (HOMO) and lowest unoccupied molecular orbital (LUMO), it is possible to more intuitively understand the electronic effects of H*-migration during the Volmer reaction mechanism, i.e., when the H*-migrates from Se to W, and the bond formation mechanism produced by H_2 during the Heyrovsky reaction mechanism. Our current calculations are very beneficial for the low energy barriers in the H*-migration and Heyrovsky steps on the 2D monolayer Janus WSSe surface during HER, leading to 2D Janus monolayer WSSe as a promising electrocatalyst. To support our current computational research on HER for 2D monolayer WSSe, we have performed natural bond orbital (NBO), The Highest Occupied Molecular Orbitals and Lowest Unoccupied Molecular Orbitals (HOMO-LUMO) calculations at the equilibrium transition states (TS 1 and TS 2) using the same M06-L DFT method. These calculations are performed to show the proper standpoint of the formation of H_2 at the active site from the perspective of the overlap of the electron charge clouds and the molecular orbitals. The NBO study delivers the most probable 'natural Lewis structure' picture of the wave function (φ), such that total information related to orbitals is selected mathematically to consider the maximum possible energy of electron density. The precise Lewis structure, which is the structure with the largest electron charge in the Lewis orbit, can be found by calculating NBO. An advantage of this orbital is that it gives information about the intra-molecular and inter-molecular interactions (i.e., connections between bonds of atoms of the molecule). Donor acceptor interactions in NBO calculations are known from second-order fock-matrix. The NBO study provides complete mathematical information about the bonding orbitals of the maximum possible energy of the electron density. The benefit of conducting this research is that it provides information about intermolecular and intramolecular interactions. The second-order Fock-matrix participates in the evolution of the donor-accepting interaction. Solving a multi-electron atomic system requires an approximation called the linear combination of atomic orbitals (LCAO approximation). A qualitative image of a molecular orbital is analyzed by

extending the molecular orbital to any absolute base of all atomic orbitals in the nucleus. Therefore, the multi-electron wave function of a molecule in a specific atomic configuration can be given by approximately extending the orbital to the molecule.

The wave function calculated from the NBO analysis is a linear combination of the W, S, Se, and H atomic orbitals of H*-migration TS1. The HOMO LUMO calculations has been performed at the optimized H*-migration TS or Volmer transition structure (i.e., TS1), as shown in Figure S5 (a) and (b). Similarly, the wave function calculated from the NBO analysis is a linear combination of the W, S, Se, H, and O atomic orbitals in the case of the Heyrovsky TS, i.e., TS2. The HOMO LUMO is obtained from at computed Heyrovsky transition structure, as shown in Figure S5 (c) and (d). The red color indicates the in-phase bonding of the orbitals, and the blue color indicates the out-of-phase bonding. The ranges of isosurface value to predict the atomic orbital overlapping around the H_2-formation (from blue to red) are set to -0.1 to 0.1.

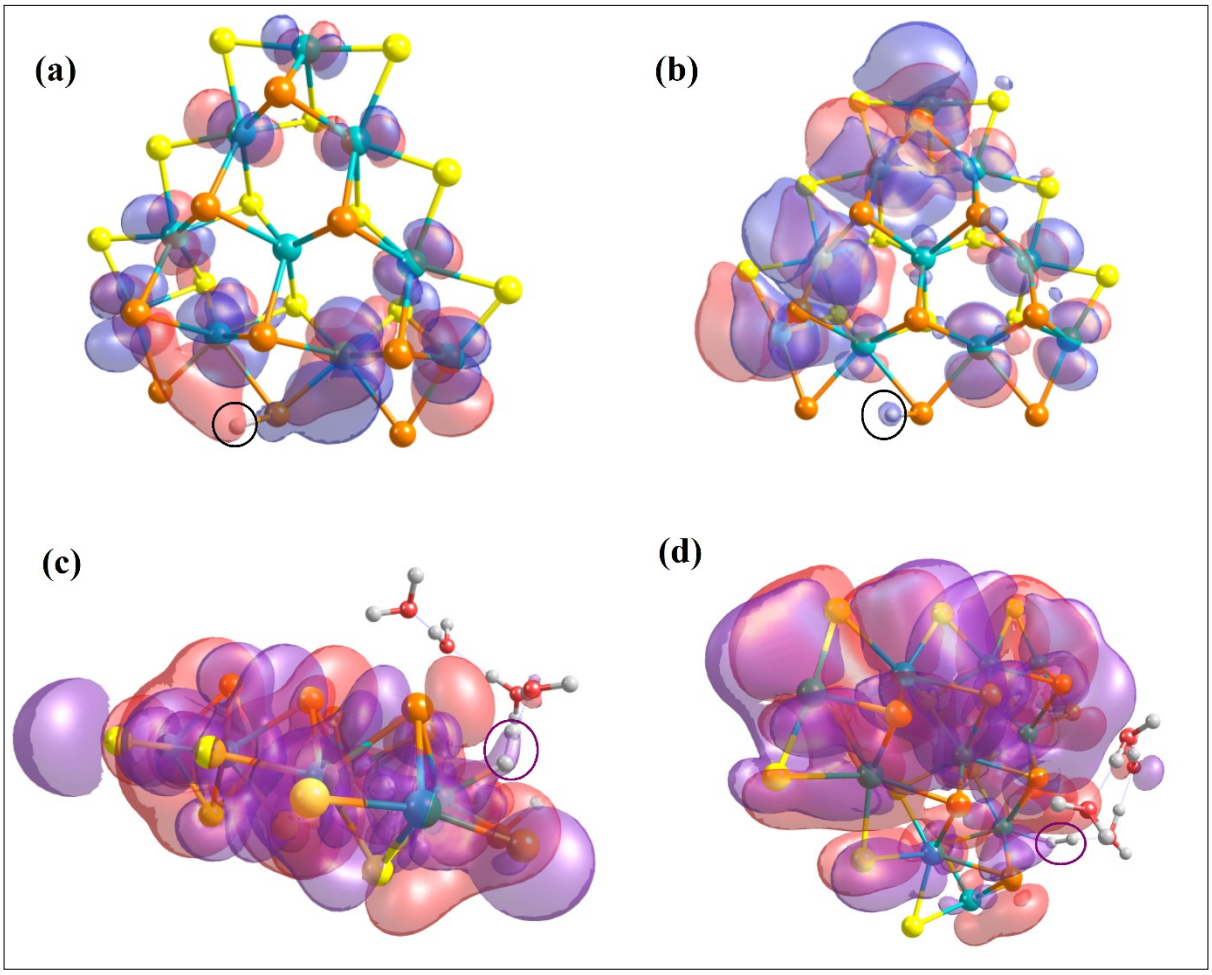

Figure S5. The equilibrium structure of (a) the HOMO of H*-migration or Volmer TS; (b) The LUMO of H* -migration TS; (c) The HOMO of Heyrovsky TS2; (d) The LUMO of Heyrovsky TS is shown

here. The positions of molecular orbitals and hydrogen participating in the subject reaction have been highlighted with dotted circles are shown here.

In the case of H*-migration TS, the HOMO-LUMO calculations indicate that the electronic wave function of the H* moves from the Se atom site to the W transition metal atom site. The light red bubble indicates that the electron in the ***s***-orbital of the H atom overlaps with the electron in the ***d***-orbital of the W atom as the electron clouds have been found in the region where the orbitals are overlapped highlighted by a black circle. The role of the electronic structure in the HER mechanism can be understood from the HOMO-LUMO calculation of the Heyrovsky transition state, as shown in Figure S5 (c-d). A better overlap of the ***s***-orbitals of the hydrogen atom attached with the W and the water cluster ($H_3O^+ + 3H_2O$) seemed in the HOMO-LUMO Heyrovsky's transition state TS2 has found, and this better overlap of the atomic orbitals during the H_2 formation in the Heyrovsky's TS2 reduces the reaction barrier. Therefore, it can be concluded that in the rate-limiting step of HER, that is, the Heyrovsky step, the stability of the atomic orbital is also one of the key features of reducing the reaction barrier. This strategy differs from well-known methods used to adjust the H_2 binding energies of TMDs or to control the acidity of the proton source. The electron cloud around the H atom in Heyrovsky TS2 is highlighted by a circle. When H_2 is precipitated, the overlap of the atomic orbitals of H and W atoms with H_3O^+ ions support this step. This is one of the reasons why the 2D monolayer Janus WSSe exhibits excellent activity against HER. The energy difference between HOMO and LUMO, also known as the HOMO-LUMO gap is used to predict the stability of transition metal-based complexes because it is the lowest energy electron excitation possible in the molecule. The HOMO and LUMO energy values of the H*-migration TS1 or Volmer TS are found at E_{HOMO}= -1.78 kcal.mol^{-1} and E_{LUMO}= -1.73 kcal.mol^{-1}, respectively. The energy required for an electron for the transition from HOMO to LUMO, $E_{GAP}= E_{LUMO} - E_{HOMO}$ = 0.05 kcal.mol^{-1}. The HOMO and LUMO energy values of Heyrovsky TS are -6.83 kcal.mol$^{-1,}$ and -5.97 kcal.mol^{-1}, respectively, as shown in Table S3. It is found that the HOMO-LUMO gap is about -0.86 kcal.mol^{-1}, which is the energy of the electron transition from HOMO to LUMO. The gentle orbital overlaps of the molecular orbitals during the H migration in the H*-migration reaction step and the H_2 formation in the Heyrovsky reaction step reveal the excellent electrocatalytic activity of the 2D monolayer Janus WSSe for HER.

Table S3. HOMO and LUMO energy and HOMO-LUMO energy gap (Eg) of all Transition states (TSs)**.**

Activation energy barrier	HOMO energy (in kcal.mol^{-1})	LUMO energy (in kcal.mol^{-1})	HOMO-LUMO energy gap (E_g) (in kcal.mol^{-1})
H* migration TS1	-1.78	-1.73	0.05
Heyrovsky TS3	-6.83	-5.97	-0.86

1 A. Ramasubramaniam, *Phys. Rev. B*, 2012, **86**, 115409.

2 S. Deng, L. Li and M. Li, *Phys. E Low-dimensional Syst. Nanostructures*, 2018, **101**, 44–49.

3 L. Ju, M. Bie, X. Tang, J. Shang and L. Kou, *ACS Appl. Mater. & Interfaces*, 2020, **12**, 29335–29343.

4 S. Pakhira and S. N. Upadhyay, *Sustain. Energy & Fuels*, 2022, **6,** 1733-1752.

5 Y. Huang, R. J. Nielsen, W. A. Goddard and M. P. Soriaga, *J. Am. Chem. Soc.*, 2015, **137**, 6692–6698.

6 P. C. Jordan, in *Chemical Kinetics and Transport*, Springer, 1979, pp. 269–323.

7 Y. Lei, S. Pakhira, K. Fujisawa, X. Wang, O. O. Iyiola, N. Perea López, A. Laura Elías, L. Pulickal Rajukumar, C. Zhou, B. Kabius, N. Alem, M. Endo, R. Lv, J. L. Mendoza-Cortes and M. Terrones, *ACS Nano*, 2017, **11**, 5103–5112.

8 J. Ekka, S. N. Upadhyay, F. J. Keil and S. Pakhira, *Phys. Chem. Chem. Phys.* 2022, **24,** 265-280.

9. A. Singh and S. Pakhira, *ACS Energy & Fuels*, 2023, **37**, 567-579.

10. S. Pakhira, V. Kumar and S. Ghosh, *Adv. Mater. Interfaces*, 2023, 2202075.